Pramāṇa Vol. 7, No. 3, 1976, pp. 194–222. © Printed in India.

General bounds on the isovector coupling constants of the weak neutral current

G RAJASEKARAN and K V L SARMA
Tata Institute of Fundamental Research, Bombay 400005

MS received 23 March 1976

Abstract. We show that experimental data on inclusive neutrino reactions can be used to obtain general bounds on the coupling constants of the isovector part of the hadronic weak neutral current provided this isovector current is related to the charged current by isospin rotation. These bounds are free from the assumption of a specific model for the neutral current as well as any dynamical assumption on the hadronic structure functions. We derive upper bounds on the coupling constants which involve only the cross sections for isospin-averaged nucleon target as well as lower bounds which require a knowledge of the cross sections for proton and neutron separately.

Keywords. Neutral current; weak interaction; isovector couplings; general bounds; octagonal inequality; variational procedure; Bjorken scaling; neutrino scattering.

1. Introduction

An entirely new class of weak interactions, namely, the neutral-current weak interaction was discovered more than two years ago (Hasert *et al* 1973). Both in the experiments at CERN as well as at FNAL (Aubert *et al* 1974, Benvenuti *et al* 1974, Barish *et al* 1975), a large number of events have been seen which can be interpreted as the following inclusive neutral-current reaction

$$\nu_\mu\,(\bar{\nu}_\mu) + \text{nucleon} \rightarrow \nu_\mu\,(\bar{\nu}_\mu) + \text{hadrons}.$$

Although other neutral-current processes such as $\bar{\nu}_\mu - e$ scattering as well as single pion production have also been seen, the inclusive processes still remain as our most copious source of data on the neutral current.

The importance of these data on the elucidation of the nature of the neutral-current interaction has prompted many calculations on the inclusive neutral-current reactions (Budny and Scharbach 1972, Pais and Treiman 1972, Riazuddin and Fayyazuddin 1972, Sehgal 1973 and 1974, Palmer 1973, Albright 1973, Paschos and Wolfenstein 1973, Pakvasa and Tuan 1974, etc.). Most of these calculations were based on specific models for the neutral-current weak interaction such as the Weinberg-Salam gauge model (Weinberg 1967 and 1972, Salam 1968) or other models (Bég and Zee 1973, Sakurai 1974, Adler and Tuan 1975, Mathur, Okubo and Kim 1975, etc.)

However, when new phenomena are experimentally discovered, it is also essential to analyze the experimental results within a sufficiently general theoretical

framework rather than interpret the data using a particular *model* of the new phenomenon. This is the point of view we have pursued in two earlier papers (Rajasekaran and Sarma 1974 *a* and *b*). In these papers the hadronic neutral current was taken to be a general combination of vector and axial vector parts each having an isoscalar piece as well as an isovector piece and thus the problem amounted to determining the four coupling constants from experimental data. Although these analyses were sufficiently general with respect to the form of the neutral current, they depended on assumptions on the hadronic structure functions following from parton model, chiral symmetry, etc.

As was recently pointed out in a brief note (Rajasekaran and Sarma 1975) it is in fact possible to derive results on the hadronic neutral current which are free from both kinds of assumptions—namely assumption of a specific model for the neutral current as well as dynamical assumptions on the hadronic structure functions. These results are in the form of bounds on the neutral-current coupling constants. Some of these results and a sketch of their derivation have already been reported in the above mentioned note which contains the general upper bounds on the isovector coupling constants as well as the model-dependent bounds involving also one of the isoscalar coupling constants. The purpose of the present paper is two-fold: to present a more complete description (with details of derivation) of the general upper bounds and to derive *lower* bounds on the isovector coupling constants.

We should also mention that now there are many excellent articles on the neutral-current reactions (Gourdin 1975, Sakurai 1975, Sehgal 1975) which review some of the model-independent results.

In section 2 we introduce the cross-sections and kinematics and derive powerful inequalities for the vector-axial-vector interference terms which play a crucial role in the subsequent considerations. For the benefit of the reader who may not be interested in the details of their derivation, these basic inequalities are summarized at the end of section 2. Section 3 presents the derivation of the general upper bounds on the isovector coupling constants which are based on the cross sections for isospin-averaged nucleon target. This section also contains a discussion of some of the weaker inequalities included for illustrative purposes (section 3.4) as well as some comments on the isovector matrix elements and chiral symmetry (section 3.5). We next show, in section 4, how one can obtain lower bounds on the isovector coupling constants if neutral current cross sections are available on proton and neutron separately. In section 5 we summarize our results and critically evaluate how good our bounds are. In the appendix, we prove by adopting a variational procedure that with the given input data, our upper bounds are the strongest that can be obtained.

2. Cross sections and Schwarz inequalities

2.1 *The interaction*

We shall assume that the interactions of the neutrino* involve only vector and axial vector covariants. This would follow, for instance, if the neutrino were a

* Neutrino here stands for the muonic-neutrino ν_μ. However, all the general results of this paper are obviously valid for ν_e also.

two-component field. The part of the effective weak interaction which is relevant for our purposes can then be written as

$$\mathcal{L}_{\text{int}} = \frac{G}{\sqrt{2}}\{\bar{\mu}\gamma_\lambda(1+\gamma_5)\,\nu\,(v_\lambda^1 + iv_\lambda^2 + a_\lambda^1 + ia_\lambda^2) + \text{h.c.}$$

$$+ \bar{\nu}\gamma_\lambda(1+\gamma_5)\,\nu\,(xv_\lambda^3 + ya_\lambda^3 + zv_\lambda^0 + wa_\lambda^0)\}, \qquad (2.1)$$

where G is the Fermi coupling constant and the vector and axial vector currents are denoted by v_λ and a_λ respectively. The superscripts 1, 2, 3 refer to the isospin index of the isovector currents and the superscript 0 refers to isoscalar currents. We have restricted the isospin of the weak currents to 0 and 1 only. The neutral-current interaction involves four coupling parameters x, y, z and w which we shall take as real, and our object is to obtain restrictions on these parameters using experimental data.

We have assumed that the isovector currents v_λ^3 and a_λ^3 belong to the same isomultiplets as the charged currents $v_\lambda^{1,2}$ and $a_\lambda^{1,2}$. This is a minimal and a natural assumption without which we cannot relate the neutral to the charged-current processes.

Also, we have ignored the strangeness-changing part of the interaction. This means that the cross-section occurring in our expressions refer to the channel $S = 0$ where S is the total strangeness of the final hadronic state. In any case, strangeness-changing part is very small for the charged current interaction and is most probably absent (in order G) for the neutral-current interaction. These remarks can be extended to the possible excitation of new quantum numbers such as charm.

2.2 *Differential cross-sections on isospin-averaged nucleon*

We now consider the inelastic cross-sections for neutrinos (denoted by ν^+) and antineutrinos (denoted by ν^-) on the isospin-averaged nucleon target $\mathcal{N}$, $\sigma_C(\nu^\pm \mathcal{N})$ which are due to the charged-current interaction and $\sigma_N(\nu^\pm \mathcal{N})$ which arise from the neutral-current interaction

$$\sigma_N(\nu^\pm \mathcal{N}) = \sigma(\nu^\pm \mathcal{N} \to \nu^\pm + \text{hadrons})$$

$$\sigma_C(\nu^\pm \mathcal{N}) = \sigma(\nu^\pm \mathcal{N} \to \mu^\mp + \text{hadrons}),$$

and by isospin-averaging we mean for instance,

$$\sigma_C(\nu^+ \mathcal{N}) \equiv \tfrac{1}{2}[\sigma(\nu p \to \mu^- + \text{hadrons}) + \sigma(\nu n \to \mu^- + \text{hadrons})].$$

The corresponding double-differential cross-sections which are functions of the standard variables Q^2 and ν, can be expressed in terms of the current-matrix-elements in the following manner

$$\frac{d^2\sigma_C(\nu^\pm \mathcal{N})}{dQ^2\,d\nu} = V_3 + A_3 \pm I_3^3 \qquad (2.2)$$

$$\frac{d^2\sigma_N(\nu^\pm \mathcal{N})}{dQ^2\,d\nu} = \frac{1}{2}(x^2 V_3 + y^2 A_3 + z^2 V_0 + w^2 A_0 \pm xyI_3^3 \pm z\,wI_0^0). \qquad (2.3)$$

Here, V_3 and A_3 stand for the contributions to the cross-sections arising from the currents v^3 and a^3 respectively; similarly V_0 and A_0 are the contributions from v^0 and a^0. The symbol $I_3{}^3$ denotes the contribution from the interference term corresponding to the product $v^3\, a^3$ while $I_0{}^0$ is that corresponding to $v^0\, a^0$. We have already used isospin invariance in writing the charged current cross sections also in terms of the third component of the isovector currents. Note that isoscalar-isovector interference terms do not occur in (2.3) since the target nucleon is averaged over isospin.

Explicitly, we have

$$\left.\begin{aligned} V_3 &= \frac{G^2}{2\pi}\frac{E'}{E}\frac{Q^2}{\nu^2}\sum_i |\langle i | l_\mu v_\mu{}^3 | p\rangle|^2 (2\pi)^3\, \delta^4(p_i - p_p - q) \\ A_3 &= \frac{G^2}{2\pi}\frac{E'}{E}\frac{Q^2}{\nu^2}\sum_i |\langle i | l_\mu a_\mu{}^3 | p\rangle|^2 (2\pi)^3\, \delta^4(p_i - p_p - q) \\ I_3{}^3 &= \frac{G^2}{2\pi}\frac{E'}{E}\frac{Q^2}{\nu^2}\sum_i 2\mathrm{Re}\{\langle i | l_\mu a_\mu{}^3 | p\rangle^* \langle i | l_\lambda v_\lambda{}^3 | p\rangle\} \\ &\quad \times (2\pi)^3\, \delta^4(p_i - p_p - q) \end{aligned}\right\} \quad (2.4)$$

and exactly analogous expressions for the isoscalar parts. Here, l_μ is the leptonic current relevant for neutrino scattering written in terms of the initial and final leptonic spinors

$$l_\mu = \bar{u}(k_2)\,\gamma_\mu(1+\gamma_5)\,u(k_1),$$

$|p\rangle$ is the spin-averaged proton† state with momentum p_p, $|i\rangle$ is a final hadronic state with momentum p_i which is summed over, and q is the four-momentum transfer of the lepton (see figure 1). We have also defined

$$Q^2 \equiv -q^2; \quad \nu \equiv \frac{q\cdot p_p}{m_p} = E - E'$$

where E and E' are the initial and final energies of the lepton in the laboratory system. We shall neglect throughout the terms involving the muon mass.

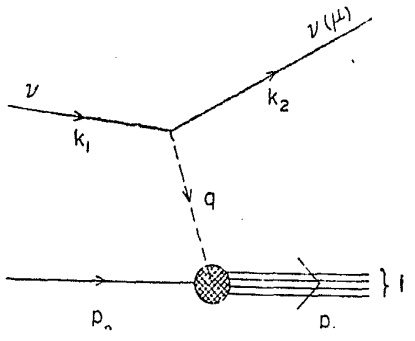

Figure 1. Inelastic neutrino scattering on a proton target giving rise to a final neutrino or muon. The symbol i denotes a final state of hadrons with total four-momentum p_i.

† Note that all our matrix elements are defined with respect to the proton target. The corresponding matrix elements for the neutron target are obtainable using charge symmetry.

Of central importance to our analysis are the inequalities relating V, A and I. By applying the Schwarz inequality to the expressions in eq. (2.4), we immediately get

$$(I_3^3)^2 \leqslant 4V_3A_3 \tag{2.5}$$

$$(I_0^0)^2 \leqslant 4V_0A_0. \tag{2.6}$$

However, from a knowledge of the helicity structure of the currents, it is possible to obtain more powerful inequalities, as we shall now proceed to show.

2.3 *Helicity decomposition*

We decompose the leptonic current into its right-handed (R), left-handed (L) and scalar (S) components and define the absorption cross sections corresponding to these helicity components of the current (Bjorken and Paschos 1970):

$$\left.\begin{aligned}
\sigma_L &= \frac{C}{2}\sum_i{}' \,|\langle i|j_x^3 - ij_y^3|p\rangle|^2 \\
\sigma_R &= \frac{C}{2}\sum_i{}' \,|\langle i|j_x^3 + ij_y^3|p\rangle|^2 \\
\sigma_S &= \frac{C}{2}\sum_i{}' \,|\langle i|j_z^3|p\rangle|^2
\end{aligned}\right\} \tag{2.7}$$

where the meaning of the primed summation symbol is

$$\sum_i{}' \equiv \sum_i (2\pi)^3\,\delta^4(p_i - p_p - q),$$

and

$$j_\mu^3 = v_\mu^3 + a_\mu^3$$

$$j_z^3 = \frac{\nu}{\sqrt{Q^2}}\left\{\left(1+\frac{Q^2}{\nu^2}\right)^{\frac{1}{2}} j_0^3 - j_z^3\right\}$$

$$C \equiv \frac{\pi}{\nu}\,\frac{1}{1-(Q^2/2m_p\nu)}$$

Here, the z axis has been chosen along $\boldsymbol{q}$.

In terms of σ_L, σ_R and σ_S the double-differential cross section can be written as

$$\frac{d^2\sigma_C(\nu=\mathcal{N})}{dQ^2\,d\nu} = \frac{G^2}{4\pi^2}\frac{E'}{E}\frac{Q^2}{\nu}\frac{1-\dfrac{Q^2}{2m_p\nu}}{1+\dfrac{Q^2}{\nu^2}}\{\alpha_1(\sigma_L+\sigma_R) + \alpha_2\sigma_S \pm \alpha_3(\sigma_L-\sigma_R)\} \tag{2.8}$$

where

$$\left.\begin{aligned}\alpha_1 &\equiv \frac{1}{4EE'}\{(E+E')^2+\nu^2+Q^2\}\\ \alpha_2 &\equiv 2\left(1-\frac{Q^2}{4EE'}\right)\\ \alpha_3 &\equiv \frac{1}{2EE'}(E+E')(\nu^2+Q^2)^{1/2}\end{aligned}\right\} \tag{2.9}$$

Next, one can study the behaviour of the matrix elements in eq. (2.7) in the lab frame, *i.e.*, $p_p = 0$. The transformation properties under rotation around the z axis and reflection in the y-z plane (see Lee and Yang 1962), allow us to arrive at the following useful forms for $\sigma_{L,R,S}$:

$$\left.\begin{aligned}\sigma_L &= 2C\sum_i{}' \overline{\sum_\lambda} \,|\langle i, \boldsymbol{q}, \lambda-1 \,|\, v_x{}^3 - a_x{}^3 \,|\, p, \boldsymbol{o}, \lambda\rangle|^2\\ \sigma_R &= 2C\sum_i{}' \overline{\sum_\lambda} \,|\langle i, \boldsymbol{q}, \lambda-1 \,|\, v_x{}^3 + a_x{}^3 \,|\, p, \boldsymbol{o}, \lambda\rangle|^2\\ \sigma_S &= C\sum_i{}' \overline{\sum_\lambda} \{|\langle i, \boldsymbol{q}, \lambda \,|\, v_s{}^3 \,|\, p, \boldsymbol{o}, \lambda\rangle|^2 + |\langle i, \boldsymbol{q}, \lambda \,|\, a_s{}^3 \,|\, p, \boldsymbol{o}, \lambda\rangle|^2\}.\end{aligned}\right\} \tag{2.10}$$

Here the notation is as follows: The state $|\, i, \boldsymbol{q}, \lambda\rangle$ denotes the final hadronic state labelled i with total 3-momentum $\boldsymbol{q}$ in the lab frame and the component of the total angular momentum along the z-axis (which is parallel to $\boldsymbol{q}$) having the value λ; the state $|\, p, \boldsymbol{o}, \lambda\rangle$ refers to the state of target proton, with zero 3-momentum, with z-component of spin to be λ; the symbol $\overline{\sum_\lambda}$ denotes the average over the target spin. Thus, as expected, σ_L and σ_R differ only by the sign of the va interference term and σ_S does not involve the interference term at all.

Substitution of eqs (2.10) into eq. (2.8) and comparison with eq. (2.2) yields the formulae:

$$\left.\begin{aligned}V_3 &= D\sum_i{}' \overline{\sum_\lambda} \left\{2\alpha_1 \,|\langle i, \boldsymbol{q}, \lambda-1 \,|\, v_x{}^3 \,|\, p, \boldsymbol{o}, \lambda\rangle|^2 + \frac{\alpha_2}{2}\,|\langle i, \boldsymbol{q}, \lambda \,|\, v_s{}^3 \,|\, p, \boldsymbol{o}, \lambda\rangle|^2\right\}\\ A_3 &= D\sum_i{}' \overline{\sum_\lambda} \left\{2\alpha_1 \,|\langle i, \boldsymbol{q}, \lambda-1 \,|\, a_x{}^3 \,|\, p, \boldsymbol{o}, \lambda\rangle|^2 + \frac{\alpha_2}{2}\,|\langle i, \boldsymbol{q}, \lambda \,|\, a_s{}^3 \,|\, p, \boldsymbol{o}, \lambda\rangle|^2\right\}\\ I_3{}^3 &= -2\alpha_3 D\sum_i{}' \overline{\sum_\lambda} 2\,\mathrm{Re}\{\langle i, \boldsymbol{q}, \lambda-1 \,|\, v_x{}^3 \,|\, p, \boldsymbol{o}, \lambda\rangle^* \times \langle i, \boldsymbol{q}, \lambda-1 \,|\, a_x{}^3 \,|\, p, \boldsymbol{o}, \lambda\rangle\}\end{aligned}\right\} \tag{2.11}$$

where

$$D \equiv \frac{G^2}{2\pi}\,\frac{E'}{E}\,\frac{Q^2}{\nu^2}\,\frac{1}{1+(Q^2/\nu^2)}$$

Notice the absence of the interference term $v_s{}^3\, a_s{}^3$ in the expression for $I_3{}^3$.

An important feature of the expressions in eq. (2.11) should be noted. In contrast to eq. (2.4), the diagonal terms and the interference term in (2.11) occur with different weighting-factors a_1, a_2, a_3. This is what leads to our improved inequality. These kinematic factors a_k defined in eq. (2.9) are never negative, and hence an application of the Schwarz inequality to eqs (2.11) yields the following inequality

$$(I_3{}^3)^2 \leq K^2\, V_3 A_3 \tag{2.12}$$

where K is defined by

$$K \equiv \frac{2a_3}{a_1} = \frac{4\,(E+E')\,(\nu^2+Q^2)^{\frac{1}{2}}}{(E+E')^2+\nu^2+Q^2}\,. \tag{2.13}$$

Since $K \leq 2$, we see that (2.12) is a better inequality than (2.5). By following exactly the same procedure with the isoscalar hadronic current $j_\mu{}^0 = v_\mu{}^0 + a_\mu{}^0$ we get the analogous inequality for the isoscalar structure functions:

$$(I_0{}^0)^2 \leq K^2\, V_0 A_0. \tag{2.14}$$

We should emphasize that the inequalities (2.12) and (2.14) are quite powerful and follow from kinematics alone, *independent of any dynamical assumption.* From these it is easy to see that

$$\frac{2}{K}\,|\,I_a{}^a\,| \leq 2\,(V_a\, A_a)^{\frac{1}{2}} \tag{2.15}$$

$$\leq V_a + A_a; \quad (a = 0, 3). \tag{2.16}$$

Obviously the inequality (2.15), which shall henceforth be referred to as the nonlinear inequality, is stronger than the inequality (2.16) to be called the linear inequality. The linear inequality for the case of charged currents was first derived by Paschos and Wolfenstein (1973).

A comparison of inequalities (2.15) and (2.16) is facilitated by figure 2, wherein, according to the nonlinear inequality the allowed values of V_3 and A_3 lie to the right of the hyperbola (marked H), while according to the weaker inequality (2.16) all the values to the right of the straight line (marked L) are allowed. More generally, we have the following linear inequalities

$$\frac{2}{K}\,|\,\lambda\mu\, I_a{}^a\,| \leqslant \lambda^2\, V_a + \mu^2\, A_a \tag{2.17}$$

where λ and μ are arbitrary real constants, and $a = 0, 3$. For various values of λ and μ we have to consider the region to the right of the tangent at various pionts on the hyperbola.

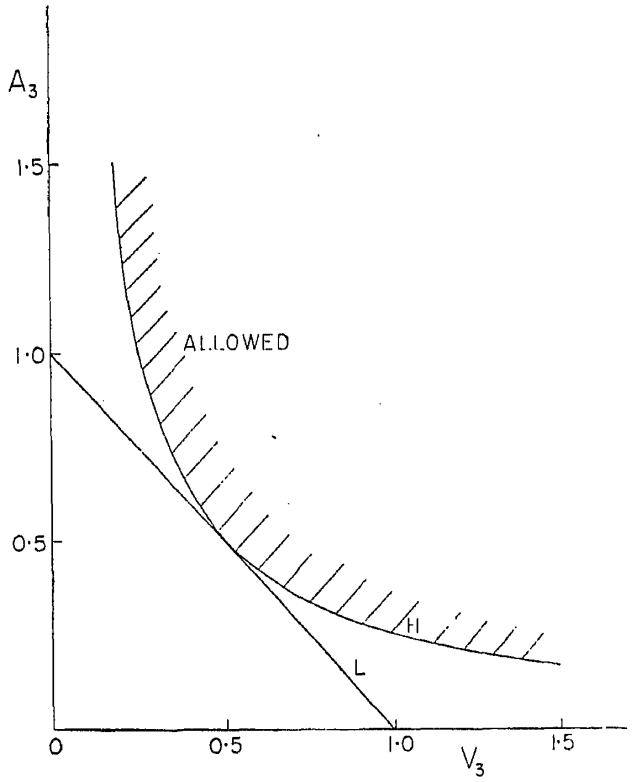

Figure 2. A comparison of the inequalities (2.15) and (2.16). Allowed values of V_3 and A_3 (in arbitrary units) according to the nonlinear inequality (2.15) lie to the right of the rectangular hyperbola (marked H) while according to the linear inequality (2.16) lie to the right of the straight line (marked L).

Using the inequality (2.17) in eqs (2.2) and (2.3) we have the lower and upper bounds on the ratios of double-differential cross sections

$$\frac{2-K}{2+K} \leqslant \frac{d^2\sigma_C\,(\nu^-\mathscr{N})/dQ^2\,d\nu}{d^2\sigma_C\,(\nu^+\mathscr{N})/dQ^2\,d\nu} \leqslant \frac{2+K}{2-K}, \tag{2.18}$$

$$\frac{2-K}{2+K} \leqslant \frac{d^2\sigma_N\,(\nu^-\mathscr{N})/dQ^2\,d\nu}{d^2\sigma_N\,(^+\nu\,\mathscr{N}\,/dQ^2\,d\nu} \leqslant \frac{2+K}{2-K}. \tag{2.19}$$

2.4 *Total cross sections and the assumption of Bjorken scaling*

Analogous to eqs (2.2) and (2.3) we have the following expressions for the total cross-sections

$$\sigma_C\,(\nu^{\pm}\mathscr{N}) = \tilde{V}_3 + \tilde{A}_3 \pm \tilde{I}_3^3 \tag{2·20}$$

$$\sigma_N\,(\nu^{\pm}\mathscr{N}) = \tfrac{1}{2}[x^2\,\tilde{V}_3 + y^2\,\tilde{A}_3 + z^2\,\tilde{V}_0 + w^2\,\tilde{A}_0 \pm xy\,\tilde{I}_3^3 \pm zw\tilde{I}_0^0], \tag{2.21}$$

where the tilde on a function means that we have performed the integration over the variables Q^2 and ν; for example

$$\tilde{V}_3 \equiv \int V_3\,dQ^2\,d\nu.$$

What are the inequalities satisfied by these integrated quantities, $\tilde{V}_3, \tilde{A}_3, \ldots$? Now the right-hand-sides of eq. (2.11) have to be integrated over Q^2 and ν,

Since a_1 and a_3 are different functions of Q^2 and ν we can get usable inequalities only by replacing a_3 by its upper bound a_1; thus we obtain the inequalities:

$$(\tilde{I}_3^3)^2 \leqslant 4\,\tilde{V}_3\,\tilde{A}_3 \tag{2.22}$$

$$(\tilde{I}_0^0)^2 \leqslant 4\,\tilde{V}_0\,\tilde{A}_0. \tag{2.23}$$

These are the analogous of the original weaker version for differential cross sections, namely eqs (2.5) and (2.6). Thus the helicity-decomposition does not seem to help us in obtaining stronger inequalities in the case of total cross sections.

We can, however, get better inequalities for the total cross sections provided we make the *dynamical assumption of scaling* (Bjorken 1969). We first define the Bjorken variables,

$$x_B \equiv \frac{Q^2}{2\,m_p \nu}, \qquad y_B = \frac{\nu}{E}. \tag{2.24}$$

Then we split up the transverse and scalar cross sections given in eq. (2.10) into the contributions from vector current, axial-vector current and the interference:

$$\left.\begin{aligned} \sigma_L &= \sigma_T^{\,v} + \sigma_T^{\,a} + \sigma_T^{va} \\ \sigma_R &= \sigma_T^{\,v} + \sigma_T^{\,a} - \sigma_T^{\,va} \\ \sigma_S &= \sigma_S^{\,v} + \sigma_S^{\,a} \end{aligned}\right\} \tag{2.25}$$

where

$$\left.\begin{aligned} \nu\sigma_T^{\,v} &\equiv \frac{2\pi}{1-x_B} \sum_i{}' \sum_\lambda{}^{-} |\langle i, q, \lambda - 1 \mid \boldsymbol{v}_x^3 \mid p, o, \lambda \rangle|^2 \\ \nu\sigma_T^{\,a} &\equiv \frac{2\pi}{1-x_B} \sum_i{}' \sum_\lambda{}^{-} |\langle i, q, \lambda - 1 \mid a_x^3 \mid p, o, \lambda \rangle|^2 \\ \nu\sigma_S^{\,v} &\equiv \frac{2\pi}{1-x_B} \sum_i{}' \sum_\lambda{}^{-} |\langle i, q, \lambda \mid a_S^3 \mid p, o, \lambda \rangle|^2 \\ \nu\sigma_S^{\,a} &\equiv \frac{2\pi}{1-x_B} \sum_i{}' \sum_\lambda{}^{-} \langle i, q, \lambda \mid a_S^3 \mid p, o, \lambda \rangle|^2 \\ \nu\sigma_T^{va} &= \frac{2\pi}{1-x_B} \sum_i{}' \sum_\lambda{}^{-} 2\,\mathrm{Re}\,\{\langle i, q, \lambda - 1 \mid v_x^3 \mid p, o, \lambda \rangle^* \\ &\qquad \times \langle i, q, \lambda - 1 \mid a_x^3 \mid p, o, \lambda \rangle\}. \end{aligned}\right\} \tag{2.26}$$

According to the assumption of Bjorken scaling for large Q^2 and ν but finite x_B, the structure functions F_1, F_2, F_3 are functions of only the variable x_B (see Bjorken

and Paschos 1970). This implies that $\nu\sigma_T^{v}$. ... $\nu\sigma_T^{va}$ depend only on x_B as can be seen from the following connection between the scaled-structure functions F's and the cross-sections defined above:

$$\left.\begin{aligned} F_1 &= \frac{m_p}{\pi}(1-x_B)(\nu\sigma_T^{v}+\nu\sigma_T^{a}) \\ F_2 - 2x_B F_1 &= \frac{2m_p}{\pi} x_B (1-x_B)(\nu\sigma_S^{v}+\nu\sigma_S^{a}) \\ F_3 &= \frac{2m_p}{\pi}(1-x_B)(\nu\sigma_T^{va}) \end{aligned}\right\} \quad (2\cdot27)$$

In terms of the scaled cross sections, we have from eq. (2.11)

$$\left.\begin{aligned} V_3 &= \frac{\beta(x_B)}{\nu}[(1-y_B+\tfrac{1}{2}y_B^2)\,\nu\sigma_T^{v}+(1-y_B)\,\nu\sigma_S^{v}] \\ A_3 &= \frac{\beta(x_B)}{\nu}[(1-y_B+\tfrac{1}{2}y_B^2)\,\nu\sigma_T^{a}+(1-y_B)\,\nu\sigma_S^{a}] \\ I_3^{3} &= \frac{\beta(x_B)}{\nu}[(y_B-\tfrac{1}{2}y_B^2)\,\nu\sigma_T^{va}], \end{aligned}\right\} \quad (2.28)$$

where for convenience we have defined

$$\beta(x_B) \equiv \frac{G^2 m_p}{\pi^2} x_B (1-x_B).$$

We can now integrate the above expressions over y_B, so that

$$\left.\begin{aligned} \tilde{V}_3 &= \int\int dQ^2 d\nu\, V_3 = \int_0^1 dx_B \int_0^1 dy_B\,(2m_p E\nu)\,V_3 \\ &= 2m_p E \int_0^1 dx_B\,\beta(x_B)\left[\frac{2}{3}\nu\sigma_T^{v}+\frac{1}{2}\nu\sigma_S^{v}\right] \\ \tilde{A}_3 &= 2m_p E \int_0^1 dx_B\,\beta(x_B)\left[\frac{2}{3}\nu\sigma_T^{a}+\frac{1}{2}\nu\sigma_S^{a}\right] \\ \tilde{I}_3^{3} &= 2m_p E \int_0^1 dx_B\,\beta(x_B)\left[\frac{1}{3}\nu\sigma_T^{va}\right]. \end{aligned}\right\} \quad (2.29)$$

With the help of the above expressions which assume the validity of Bjorken scaling, we can now derive a strong inequality. For this, we first note that Schwarz inequality applied to eq. (2.26) reads as

$$\sigma_T^{va} \leqslant 2(\sigma_T^{v}\,\sigma_T^{a})^{1/2}. \quad (2.30)$$

For the integrated functions, since the scalar-contributions are positive definite we have

$$\tilde{V}_3\tilde{A}_3 \geqslant (2m_pE)^2 \int_0^1 dx_B\, \beta(x_B) \left[\frac{2}{3}\nu\sigma_T{}^v\right] \int_0^1 dx_B\, \beta(x_B) \left[\frac{2}{3}\nu\sigma_T{}^a\right]$$

$$\geqslant \left[2m_pE \int_0^1 dx_B\, \beta(x_B)\, \frac{2}{3}\, \nu\, (\sigma_T{}^v\, \sigma_T{}^a)^{1/2}\right]^2.$$

On making use of (2.30) we at once obtain the inequality

$$(\tilde{I}_3{}^3)^2 \leqslant \tilde{V}_3\tilde{A}_3, \text{ and similarly,} \tag{2.31}$$

$$(\tilde{I}_0{}^0)^2 \leqslant \tilde{V}_0\tilde{A}_0. \tag{2.32}$$

These are the improved inequalities for total cross sections which may be compared with inequalities (2.22) and (2.23). An inequality closely related to (2.31) was derived and used by Paschos and Zakharov (1973).

For the total cross sections also we can write down the linearized versions of the inequalities (2.22), (2.23), (2.31) and (2.32):

$$\frac{2}{K_t} \mid \lambda\mu\, \tilde{I}_a{}^a \mid \leqslant \lambda^2\, \tilde{V}_a + \mu^2\, \tilde{A}_a; \quad (a = 0, 3), \tag{2.33}$$

where λ and μ are arbitrary real numbers and $K_t = 1$ or 2 depending on whether Bjorken scaling is used or not. Again we can derive from (2.33) with $K_t = 1$ the well-known result

$$\frac{1}{3} \leqslant \frac{\sigma_{C,N}(\nu^- \mathscr{N})}{\sigma_{C,N}(\nu^+ \mathscr{N})} \leqslant 3. \tag{2.34}$$

The case $K_t = 2$, on the other hand, does not lead to any nontrivial bound on the ratio of total cross sections.

In summary, we have derived the following inequalities:

(i) For the differential cross sections, strong inequalities;

$$\mid I_a{}^a \mid \leqslant K(V_aA_a)^{1/2}; \quad (a = 0, 3),$$

where K is a kinematical function defined in eq. (2.13).

(ii) For the total cross sections,

$$\mid \tilde{I}_a{}^a \mid \leqslant K_t(\tilde{V}_a\tilde{A}_a)^{1/2}; \quad (a = 0, 3),$$

where, $K_t = 1$ corresponds to a strong inequality based on the assumption of scaling, and $K_t = 2$ gives a weak inequality free from any dynamical assumption. Further, we have linear versions of each of these inequalities given in (2.17) and (2.33).

3. Upper bounds on the isovector coupling constants

3.1. *Derivation of the main inequality*

It is convenient to define the sums and differences of the double differential cross

›r the neutrino (ν^+) and antineutrino (ν^-) on the isospin-averaged
$\mathcal{N}$):

$$\sigma_{C,N} \equiv \frac{1}{2}\left[\frac{d^2\sigma_{C,N}(\nu^+\mathcal{N})}{dQ^2\,d\nu} + \frac{d^2\sigma_{C,N}(\nu^-\mathcal{N})}{dQ^2\,d\nu}\right]$$

$$\sigma_{C,N} \equiv \frac{1}{2}\left[\frac{d^2\sigma_{C,N}(\nu^+\mathcal{N})}{dQ^2\,d\nu} - \frac{d^2\sigma_{C,N}(\nu^-\mathcal{N})}{dQ^2\,d\nu}\right]. \tag{3.1}$$

(2.2) and (2.3) we have

$$= V_3 + A_3 \tag{3.2}$$

$$_C = I_3^3 \tag{3.3}$$

$$= \tfrac{1}{2}[x^2 V_3 + y^2 A_3 + z^2 V_0 + w^2 A_0] \tag{3.4}$$

$$_N = \tfrac{1}{2}[xy I_3^3 + zw I_0^0]. \tag{3.5}$$

he bounds, we shall use only the positivity of V_3, A_3, V_0 and A_0 and ties derived in section 2:

$$^3)^2 \leqslant K^2 V_3 A_3 \tag{3.6}$$

$$^0)^2 \leqslant K^2 V_0 A_0 \tag{3.7}$$

kinematical factor K has been defined in eq. (2.13). We may first lowing consequences of the linearized version of the inequalities (3.6)

$$|\Delta_C| \leqslant K\Sigma_C \tag{3.8}$$

$$|\Delta_N| \leqslant K\Sigma_N \tag{3.9}$$

the same content as inequalities (2.18) and (2.19).

tion we would like to pose now is as follows:

four equations (3.2)–(3.5) and the two inequalities (3.6) and (3.7), information obtainable on the parameters x, y, z and w?

let us first study the information provided by the data on charged ss sections. Using eqs (3.2), (3.3) and (3.6) we eliminate A_3 and inequality for V_3:

$$(V_3^2 - V_3\Sigma_C) + \Delta_C^2 \leqslant 0$$

be rewritten as

$$(V_3 - V_{3m})(V_3 - V_{3M}) \leqslant 0 \tag{3.10}$$

$$_{3m} = \frac{\Sigma_C}{2}\left[1 - \left(1 - \frac{4\Delta_C^2}{K^2\Sigma_C^2}\right)^{\frac{1}{2}}\right];$$

$$_{3M} = \frac{\Sigma_C}{2}\left[1 + \left(1 - \frac{4\Delta_C^2}{K^2\Sigma_C^2}\right)^{\frac{1}{2}}\right]. \tag{3.11}$$

Inequality (3.10) implies that V_3 (and similarly A_3 also) should satisfy the constraints:

$$V_{3m} \leqslant V_3 \leqslant V_{3M}$$
$$V_{3m} \leqslant A_3 \leqslant V_{3M} . \tag{3.12}$$

A discussion of the inequality (3.10) is given separately in subsection 3.5.

We now go back to eqs. (3.4) and (3.5). Multiplying eq. (3.4) by K and eq. (3.5) by 2, and adding as well as subtracting the resulting equations, we get

$$K(2\Sigma_N - x^2 V_3 - y^2 A_3) \pm 2(2\triangle_N - xy\triangle_C)$$
$$= K(z^2 V_0 + w^2 A_0) \pm 2zwI_0^0 . \tag{3.13}$$

By virtue of (3.7), the right-hand-side of (3.13) is positive. Hence, rewriting the left-hand-side of (3.13) using (3.2), we have

$$K[2\Sigma_N - y^2 \Sigma_C - (x^2 - y^2) V_3] \pm 2(2\triangle_N - xy\triangle_C) \geqslant 0. \tag{3.14}$$

Note that we have, in effect used the linear version of (3.7), namely (2.17). Clearly, V_3 in (3.14) can be replaced by the minimum value V_{3m} for $x^2 > y^2$ and by the maximum value V_{3M} for $x^2 < y^2$. Thus the solution to our problem can be given in the form of an inequality involving the coupling x and y and measurable experimental quantities [Rajasekaran and Sarma (1975)] :

$$x^2 + y^2 - \left(1 - \frac{4\triangle_C{}^2}{K^2\Sigma_C{}^2}\right)^{\frac{1}{2}} | x^2 - y^2 | + \frac{4}{K\Sigma_C} | 2\triangle_N - xy\triangle_C | \leqslant \frac{4\Sigma_N}{\Sigma_C} . \tag{3.15}$$

We shall also write down explicitly the corresponding inequality for the total cross sections:

$$x^2 + y^2 - \left(1 - \frac{4\tilde{\triangle}_C{}^2}{K_t{}^2\tilde{\Sigma}_C{}^2}\right)^{\frac{1}{2}} | x^2 - y^2 | + \frac{4}{K_t\tilde{\Sigma}_C} | 2\tilde{\triangle}_N - xy\tilde{\triangle}_C | \leqslant \frac{4\tilde{\Sigma}_N}{\tilde{\Sigma}_C} \tag{3.15'}$$

wherein, one sets $K_t = 1$ if one wishes to assume the validity of Bjorken scaling, whereas if scaling were not assumed one sets $K_t = 2$ (see the end of section 2). Here the tilde signifies [as in eq. (2.20)] that the integrations over Q^2 and ν have been performed and thus the quantities involve the total cross sections; for instance,

$$\tilde{\Sigma}_C = \tilde{V}_3 + \tilde{A}_3 = \tfrac{1}{2}[\sigma_C(\nu^+ \mathscr{N}) + \sigma_C(\nu^- \mathscr{N})] .$$

It should be noted that the inequality (3.15) or (3.15') follows from completely model-independent considerations. A natural question arises whether one could derive a better result by following a different procedure. We prove in the appendix that with the given input on neutrino cross sections, the inequality (3.15) is the best that can be obtained.

3.2 *The octagonal region*

When the two modulii are unravelled one finds that the inequality (3.15) implies that the values of x and y are confined to the interior of an octagon. The eight straight lines of the octagon are defined by the equation,

$$(1 + \epsilon_1\rho)^{\frac{1}{2}} x + \epsilon_2 (1 - \epsilon_1\rho)^{\frac{1}{2}} y + 2\epsilon_3 \left[\frac{K\Sigma_N + 2\epsilon_2\triangle_N}{K\Sigma_C}\right]^{\frac{1}{2}} = 0 \tag{3.16}$$

where

$$\rho = \left[1 - \frac{4\triangle_C^2}{K^2 \Sigma_C^2}\right]^{\frac{1}{2}},$$

$$\epsilon_1 = -1, \quad \text{for} \quad x^2 > y^2$$

$$= +1, \quad \text{for} \quad x^2 < y^2$$

$$\epsilon_i = \pm 1, \quad \text{for} \quad i = 2, 3.$$

The signs of ϵ_k distinguish the eight straight lines. If, however, $\rho = 0$ then the octagon will become a rectangle. Clearly the inequality (3.15′) also leads to an octagon of the type defined above and for this reason we shall refer to (3.15) and (3.15′) as the octagonal inequalities.

We note that detailed neutrino data on differential cross sections are not available at the present time. Therefore for the sake of plotting we shall only deal with the inequality referring to the total cross sections, and for this purpose consider the CERN Gargamelle data:

$$\left.\begin{aligned} R_C &\equiv \frac{\sigma_C(\nu^- \mathscr{N})}{\sigma_C(\nu^+ \mathscr{N})} = 0{\cdot}38 \pm 0{\cdot}02, \text{ (Eichten } et\ al \text{ 1973)} \\ r &\equiv \frac{\sigma_N(\nu^+ \mathscr{N})}{\sigma_C(\nu^+ \mathscr{N})} = 0{\cdot}22 \pm 0{\cdot}03, \text{ (Hasert } et\ al \text{ 1974)} \\ \bar{r} &\equiv \frac{\sigma_N(\nu^- \mathscr{N})}{\sigma_C(\nu^- \mathscr{N})} = 0{\cdot}55 \pm 0{\cdot}07, \text{ (Morfin, 1975).} \end{aligned}\right\} \quad (3.17)$$

These measurements utilize the Freon target and a neutrino beam whose spectrum extends up to about 10 GeV. It is important to note that these data were obtained after effecting a cut on the minimum total energy of the final hadrons and therefore do not refer to the true values of the total cross sections. Moreover the energy spectra of neutrinos and antineutrinos are not identical. Since we would like only to illustrate the efficacy of the inequalities derived in this paper, we shall ignore the above complications in the experimental data and also ignore the quoted errors in eq. (3.17).

Data on total cross sections are also available at much higher energies coming from FNAL (Aubert *et al* 1974, Benvenuti *et al* 1974, Barish *et al* 1975). However, due to the possible onset of new effects such as the excitation of new quantum numbers at FNAL energies, we shall restrict ourselves to the Gargamelle data.

The octagon in the xy-plane implied by the eq. (3.16) is plotted in figure 3 using the median values of the data given in eq. (3.17), for two cases. The inner octagon is for the case of $K_t = 1$ and follows from the assumption of Bjorken scaling whereas the outer octagon is for the case of $K_t = 2$ which is independent of any such dynamical assumption. The allowed values of x and y are constrained to lie within the inner (outer) octagon if scaling is (is not) assumed.

In general, the octagon will be oriented asymmetrically with respect to the coordinate axes with a tilt. However, for the input data used, because $(\tilde{\triangle}_N/\tilde{\Sigma}_N)$ is very small ($\simeq 0{\cdot}03$) this tilt is slight and hence is barely visible in our plot. Secondly, it may be noted that if R_C defined in eq. (3.17) has the value 1/3 the inner octagon will reduce to a rectangle.

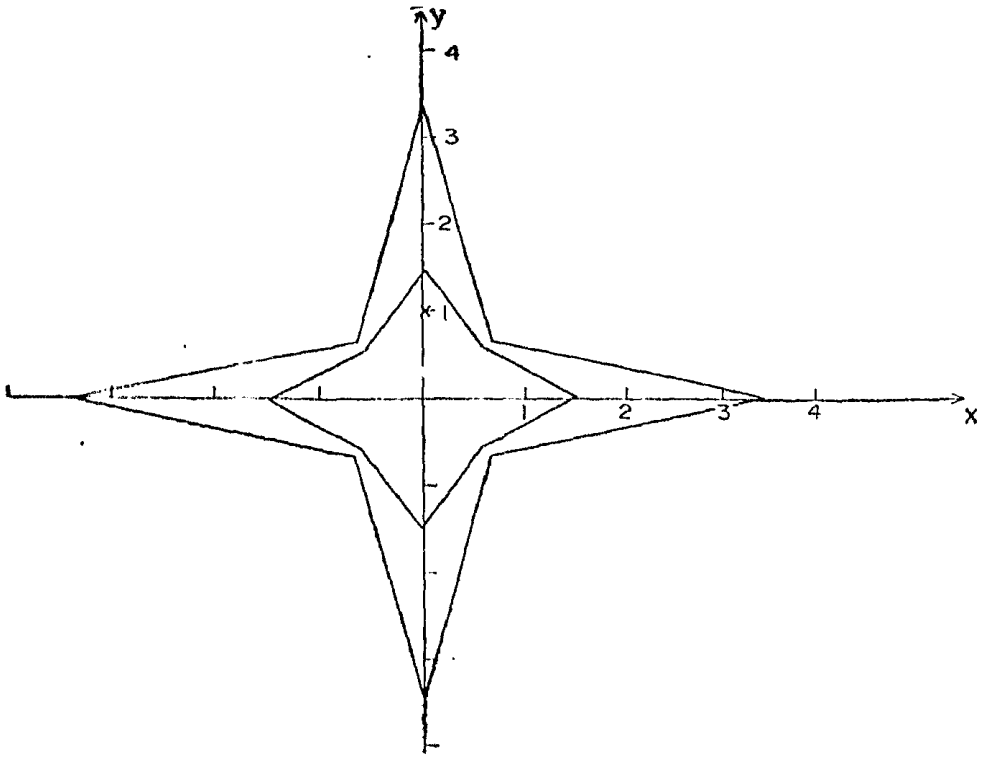

Figure 3. The region within which the allowed values of the isovector couplings x and y should lie according to the octagonal inequality (3.15'). CERN data on neutrino and antineutrino total cross sections are used. The outer octagon refers to the case $K_t = 2$, and the inner octagon to the case $K_t = 1$ which assumes Bjorken scaling. The point marked (X) refers to the Weinberg-Salam model.

We may also point out here that for Weinberg-Salam model (with the effects of strange and possible charmed hadrons ignored) the isoscalar axial vector current $wa_\lambda{}^0$ can be dropped, in which case, eqs (3.3) and (3.5) imply that x and y lie on the rectangular hyperbola:

$$xy/\Delta_C = -2\Delta_N. \tag{3.18}$$

The Weinberg-Salam point $y = 1$, $x = (2\tilde{\Delta}_N/\tilde{\Delta}_C)$ for the median values of the data of eq. (3.17) is indicated in figure 3 by a cross (X).

3.3 *Possible improvement by the use of electron-scattering data*

So far we have used only the neutrino-scattering data. Since v^3 is a part of the electromagnetic current by the conserved-vector-current hypothesis, we obviously have the bound (Paschos and Wolfenstein 1973)

$$V_3 \leqslant V_{em} = \frac{G^2}{4\pi^2 a^2} Q^4 \frac{d^2\sigma_{em}(e\mathscr{N})}{dQ^2\, dv}. \tag{3.19}$$

Here the double-differential cross section on the right refers to the inelastic electron scattering on the isospin-averaged nucleon target and the factor in front arises from the fact that electron-scattering involves the fine structure constant a and the photon propagator $1/Q^2$ whereas neutrino-scattering involves G.

If the data on electron-scattering and neutrino scattering (by charged currents) are such that $V_{em} \leqslant V_{3M}$, then V_{em} provides a better upper bound for V_3 than V_{3M}. Therefore for $x^2 < y^2$, for the maximum value of V_3 in the inequality (3.14)

we may use V_{em}. As a result, the allowed region for $x^2 < y^2$ is restricted by the following inequality:

$$y^2\Sigma_C - (y^2 - x^2)\, V_{em} + \frac{2}{K} \mid 2\Delta_N - xy\ \Delta_C \mid \leq 2\,\Sigma_N\ ; \tag{3·20}$$

while for $x^2 > y^2$, the inequality (3.15) is left unaltered.

For the numerical work, we shall again be concerned only with the integrated quantities. Defining $\tilde{V}_{em}$ as in section 2.4 as the integral of the right-hand-side of (3.19) over Q^2 and ν, and using the electron-scattering data (Kendall 1972) as well as the neutrino-scattering data (Eichten *et al* 1973), we get, neglecting errors,

$$\frac{\tilde{V}_{em}}{\sigma_C\,(\nu + \mathcal{N})} = 0{\cdot}36. \tag{3.21}$$

For comparison, we give here the values of $\tilde{V}_{3m}$ and $\tilde{V}_{3M}$ derived from eq. (3.17)

$$\frac{\tilde{V}_{3m}}{\sigma_C\,(\nu + \mathcal{N})} = 0{\cdot}19, \qquad \frac{\tilde{V}_{3M}}{\sigma_C\,(\nu + \mathcal{N})} = 0{\cdot}50. \tag{3.22}$$

For these values, we see that $\tilde{V}_{em} < \tilde{V}_{3M}$ so that we can use the improved version (3.20) for $x^2 < y^2$. The improvement achieved thereby is indicated in figure 4 for the case of $K_t = 1$. Although the boundary given by eq. (3.20) is a pair of conic sections, it is not far from a quartet of straight lines for the actual numerical values used. However, because of sizeable errors in the above experimental numbers we cannot decide at the present time which of the two quantities $\tilde{V}_{3M}$ and $\tilde{V}_{em}$ is in fact the larger one, and hence whether the apparent improvement depicted in figure 4 is a genuine one.

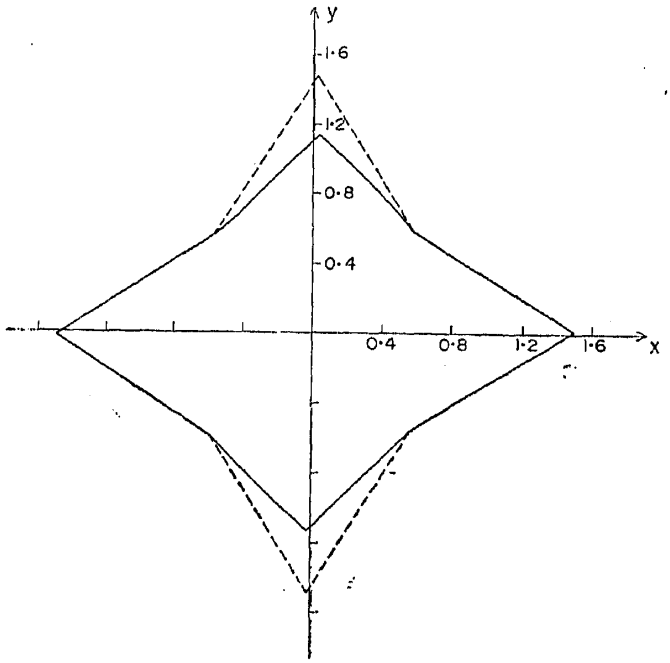

Figure 4. Improvement of the octagon for $K_t = 1$ by the use of electron scattering data. The figure in solid line is the allowed region obtained for the case $K_t = 1$ by using the eN data. For comparison the inner octagon of figure 3 is indicated here by dotted line, which coincides with the solid line for $\mid x \mid > \mid y \mid$.

3.4 *Some inequalities weaker than the octagonal inequality*

Here we shall consider some simple inequalities which may be of special interest and help to put the octagonal inequality in perspective. It is convenient to develop the discussion in the following three stages:

(A) If in the expression for Σ_N in eq. (3.4) one ignores the last two isoscalar terms and utilizes the bounds (3.12) satisfied by V_3 and A_3, one gets

$$\begin{aligned} 2\Sigma_N &\geqslant x^2 V_3 + y^2 A_3 \\ &\geqslant (x^2 + y^2)\, V_{3m}. \end{aligned} \tag{3.23}$$

Therefore the values of x and y are confined to the interior of a circle in the xy plane. For the data on total cross sections (for using which one replaces in the above expression Σ_N by $\tilde{\Sigma}_N$, etc.) given in eq. (3.17) assuming scaling, this circle is shown in figure 5.

(B) We observe that when V_3 takes its maximum value V_{3M}, because of eq. (3.2) A_3 must equal V_{3m}, and *vice versa*. Therefore instead of the second step in eq. (3.23) we may consider two possibilities depending on whether $(x^2 - y^2)$ is positive or negative:

$$\begin{aligned} 2\Sigma_N &\geqslant x^2 V_3 + y^2 (\Sigma_C - V_3) \\ &\geqslant \begin{cases} (x^2 - y^2)\, V_{3m} + y^2 \Sigma_C, & \text{for } x^2 \geqslant y^2 \\ (x^2 - y^2)\, V_{3M} + y^2 \Sigma_C, & \text{for } x^2 \leqslant y^2 \end{cases} . \end{aligned} \tag{3.24}$$

Thus we obtain the two inequalities defining a pair of intersecting ellipses in the xy plane, which are also shown in figure 5 for the data on total cross sections.

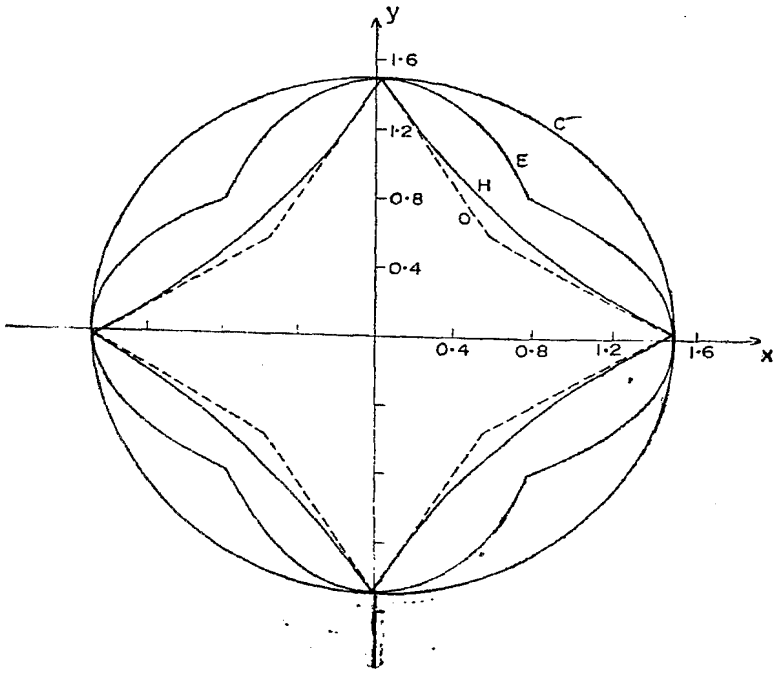

Figure 5. Content of some weak inequalities assuming Bjorken scaling ($K_t = 1$). The curve C is the circle of the inequality (3.23), curve E is the pair of ellipses on (3.24), curve H denotes the two pairs of hyperbolas of (3.26). Dotted curve O is the octagon of (3.15′) shown for the sake of comparison.

(C) Further tightening of the above inequalities (3.23) and (3.24) occurs when use is made of the linear inequality (2.17) satisfied by I_0^0;

$$2\Sigma_N - x^2 V_3 - y^2 A_3 \geqslant \frac{2}{K} | zwI_0^0 | . \tag{3.25}$$

Using the lower bounds on V_3 and A_3 and eqs (3.3) and (3.5), one obtains

$$x^2 + y^2 - \frac{2}{KV_{3m}} | 2\Delta_N - xy\, \Delta_C | \leqslant \frac{2\Sigma_N}{V_{3m}} \tag{3.26}$$

which represents in the xy plane a domain bounded by two pairs of hyperbolas as shown in figure 5. Note that if $\Delta_C = KV_{3m}$ the hyperbolas degenerate into two pairs of straight lines.

As a next step, in view of the observation made in paragraph (B), improvement over the hyperbola inequalities (3.26) leads to the octagonal inequality (3.15) (shown by broken line in figure 5), which of course is the strongest as it uses the non-linear inequality (2.15) for I_3^3 and the linear inequality (2.17) for I_0^0.

3.5 *A comment on the isovector structure functions and chiral symmetry*

Here we digress from our main enquiry for a brief discussion of the values of the isovector structure functions V_3 and A_3 which are obtainable from the data on charged-current cross sections. We recall that the bounds (3.12) provide us with model-independent information on V_3 and A_3 and do not even depend on the assumption of scaling.

The following bound on the difference between V_3 and A_3 follows from the inequality (3.10):

$$\frac{| V_3 - A_3 |}{V_3 + A_3} \leqslant \left(1 - \frac{4\Delta_C^2}{K^2 \Sigma_C^2}\right)^{\frac{1}{2}} \tag{3.27}$$

and it can be used to test chiral symmetry (see Paschos and Zakharov 1973, Rajasekaran and Sarma 1974 *b*). For total cross sections, one observes that under the assumption of scaling (K is replaced by unity) chiral symmetry becomes exact, *i.e.* $\tilde{V}_3 = \tilde{A}_3$, only if $2 | \tilde{\Delta}_C | = \tilde{\Sigma}_C$.

To elaborate further we rewrite the quadratic inequality (3.10) for the integrated quantities $\tilde{V}_3$ and $\tilde{A}_3$;

$$\left(\frac{\tilde{V}_3}{\tilde{\Sigma}_C}\right)^2 - \frac{\tilde{V}_3}{\tilde{\Sigma}_C} + \frac{1}{K_t^2}\left(\frac{1 - R_C}{1 + R_C}\right)^2 \leqslant 0 \tag{3.28}$$

where R_C is the ratio of charged-current total cross sections

$$R_C \equiv \frac{\sigma_C(\nu^- \mathcal{N})}{\sigma_C(\nu^+ \mathcal{N})} . \tag{3.29}$$

The content of this inequality is displayed in figure 6 as a plot of $(2\tilde{V}_3/\tilde{\Sigma}_C)$ *versus* R_C, for both the cases $K_t = 1$ (full line) and $K_t = 2$ (broken line). In each case there are two values of the ordinate for a given value of R_C and these denote the

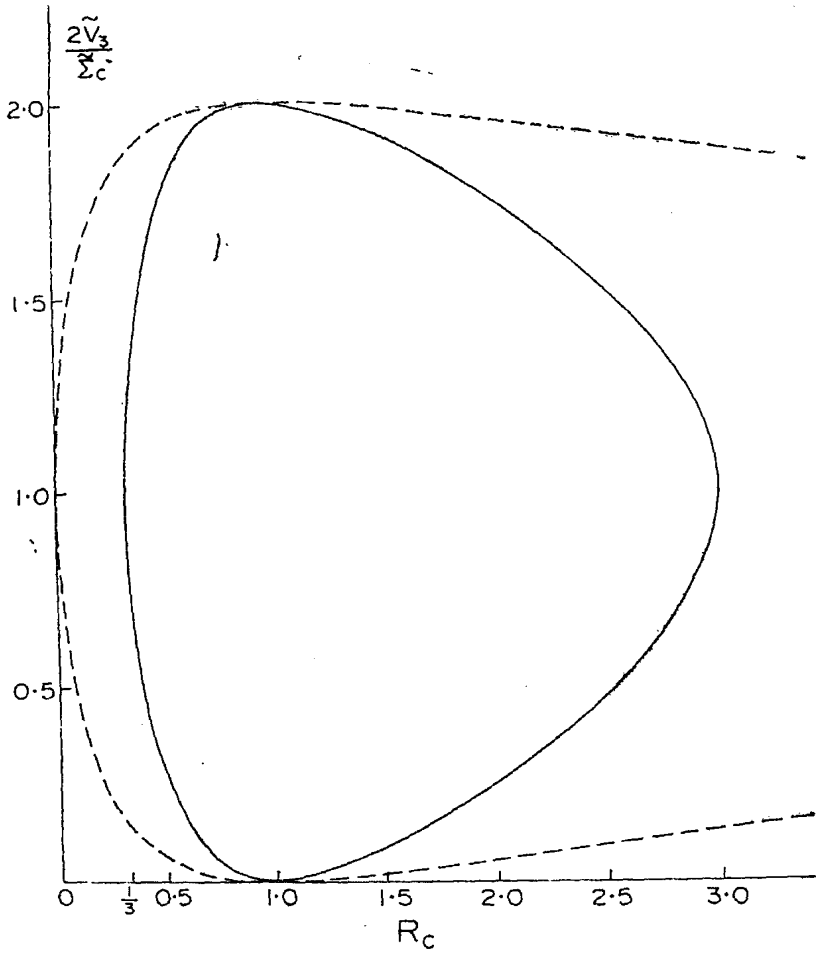

Figure 6. Allowed region of the values of $(2\tilde{V}_3/\tilde{\Sigma}_C)$ as a function of R_C according to the inequality (3.27). Broken line corresponds to $K_t = 2$, and solid line to the case $K_t = 1$ when scaling is assumed. This plot is also valid for $(2\tilde{A}_3/\tilde{\Sigma}_C)$ as the ordinate.

maximum and minimum values corresponding to the bounds (3.12). For the case of $K_t = 1$ (*i.e.*, scaling) we see that as R_C approaches 1/3 or 3, the value of $(2\tilde{V}_3/\tilde{\Sigma}_C)$ approaches unity and hence $\tilde{V}_3$ approaches $\tilde{A}_3$.

An interesting feature of these inequalities may be pointed out here. Since the bounds on R_C given by (2.34) are directly obtained from the linear inequality (2.33), the closeness of the experimental value of R_C to the lower bound 1/3 suggests that the linear inequality (2.33) with $a = 3$, $\lambda = \mu = 1$ and $K_t = 1$ is close to being saturated. In other words, referring to figure 2, $\tilde{V}_3$ and $\tilde{A}_3$ lie very close to the straight line L. But we already know that the physical values of $\tilde{V}_3$ and $\tilde{A}_3$ have to lie to the right of the hyperbola H (given by the quadratic inequality) anp cannot lie on the straight line L unless $\tilde{V}_3 = \tilde{A}_3$. So we conclude that $\tilde{V}_3 \approx \tilde{A}_3$. Thus, from the single experimental datum: $R_C \approx 1/3$, one can infer not only that the quadratic inequality (2.31) is very nearly saturated but also that chiral symmetry is approximately correct.

However, it is evident from figure 6 that the approach towards the chiral symmetric point is rather "slow". Even for small departures from $R_C = 1/3$ the deviations from exact chiral symmetry are sizable; for instance, if $R_C = 0{\cdot}38$ the right hand side of the inequality (3.27) (for total cross sections with $K_t = 1$) turns out to be 0·44.

4. Lower bounds on the isovector coupling constants

The bounds given in the previous section are in the nature of upper bounds for the magnitudes of the isovector coupling constants x and y. For, given the isospin-averaged nucleon cross sections alone, we cannot rule out the case $x = y = 0$, *i.e.*, the possibility that the neutral current is a pure isoscalar. On the other hand, since the difference between cross sections for proton and neutron targets arises from isovector-isoscalar interference term, it is clear that this difference can be used to set lower bounds on $|x|$ and $|y|$. This is the purpose of the present section.

The neutral-current cross sections for proton target and neutron target can be written as

$$\frac{d^2\sigma_N(\nu^{\pm}p)}{dQ^2\,d\nu} = \tfrac{1}{2}\Big[x^2V_3 + y^2A_3 + z^2V_0 + w^2A_0 \pm xyI_3^3 \pm zwI_0^0 \pm xwI_3^0 \pm yzI_0^3 + (xzI_{30} + ywI^{30})\Big]$$

$$\frac{d^2\sigma_N(\nu^{\pm}n)}{dQ^2\,d\nu} = \tfrac{1}{2}\Big[x^2V_3 + y^2A_3 + z^2V_0 + w^2A_0 \pm xyI_3^3 \pm zwI_0^0 \mp xwI_3^0 \mp yzI_0^3 - (xzI_{30} + ywI^{30})\Big] \tag{4.1}$$

where $\nu^{\pm}$ denote neutrino and antineutrino as before, and all the interference terms are defined in a manner similar to eq. (2.3)—the lower (upper) index of of the interference term denotes the isospin character of the vector (axial vector) current—for instance, I_k^l is the interference arising from v_λ^k and a_λ^l. Similar to the definitions of Σ_N and Δ_N in eq. (3.1) in terms of the sums of cross sections for p and n, we now define S_N and D_N in terms of the differences of p and n cross sections:

$$S_N \equiv \tfrac{1}{4}[\partial\sigma_N(\nu^+p) - \partial\sigma_N(\nu^+n) + \partial\sigma_N(\nu^-p) - \partial\sigma_N(\nu^-n)]$$

$$D_N \equiv \tfrac{1}{4}[\partial\sigma_N(\nu^+p) - \partial\sigma_N(\nu^+n) - \partial\sigma_N(\nu^-p) + \partial\sigma_N(\nu^-n)], \tag{4.2}$$

where the symbol ∂ stands for the double differential $d^2/dQ^2\,d\nu$. From eqs (4.1) and (4.2) we get

$$S_N = \tfrac{1}{2}(xzI_{30} + ywI^{30})$$

$$D_N = \tfrac{1}{2}(xwI_3^0 + yz\,I_0^3). \tag{4.3}$$

The interference terms occurring here satisfy the following inequalities:

$$|I_3^0| \le K(V_3A_0)^{1/2}; \qquad |I_0^3| \le K(V_0A_3)^{1/2} \tag{4.4}$$

$$|I_{30}| \le 2(V_3V_0)^{1/2}; \qquad |I^{30}| \le 2(A_3A_0)^{1/2} \tag{4.5}$$

where K is the same kinematical factor defined in eq. (2.13). It should be noted that whereas the (va) interference terms are bounded by the more powerful inequalities in (4.4), we should be content with the simple Schwarz inequalities (4.5) for the (vv) and the (aa) interference terms.

Before we proceed to derive the bounds involving S_N and D_N, we shall obtain constraints on the isoscalar parts which involve only isospin-averaged cross sections. By combining eqs (3.3), (3.5) and (3.7) we get the inequality,

$$\frac{1}{K^2}(2\triangle_N - xy\triangle_C)^2 \leqslant z^2w^2\, V_0A_0, \tag{4.6}$$

and using this in eq. (3.4) we obtain

$$(z^2V_0)^2 - z^2\, V_0\,(2\Sigma_N - x^2\, V_3 - y^2\, A_3) + \frac{1}{K^2}(2\triangle_N - xy\triangle_C)^2 \leqslant 0. \tag{4.7}$$

Eliminating A_3 with the help of eq. (3.2) and replacing V_3 by its extreme values (3.12) one gets

$$(z^2V_0)^2 - z^2V_0\, M + \frac{1}{K^2}(2\triangle_N - xy\triangle_C)^2 \leqslant 0 \tag{4.8}$$

where

$$\begin{aligned} M &= 2\Sigma_N - y^2\,\Sigma_C - (x^2 - y^2)\, V_{3m}, \quad \text{for } x^2 > y^2 \\ &= 2\Sigma_N - y^2\,\Sigma_C - (x^2 - y^2)\, V_{3M}, \quad \text{for } x^2 < y^2. \end{aligned} \tag{4.9}$$

The content of this quadratic inequality (4.8) is to force the variable $(z^2\, V_0)$ to lie between the two roots γ_1 and γ_2;

$$\gamma_1 \leqslant z^2V_0 \leqslant \gamma_2 \tag{4.10}$$

where

$$\gamma_{2,1} = \tfrac{1}{2}M \pm \tfrac{1}{2}\left[M^2 - \frac{4}{K^2}(2\triangle_N - xy\,\triangle_C)^2\right]^{1/2}. \tag{4.11}$$

Obviously, w^2A_0 satisfies the same constraints as (4.10). It should be noted that in contrast to the bounds on the isovector parts given in (3.12), the constraints (4.10) on the isoscalar parts depend also on the coupling strengths x and y.

We shall make use of (4.10) in deriving the bounds involving S_N and D_N. Using the inequalities (4.4) and (4.5) we obtain from eq. (4.3)

$$\begin{aligned} 2\,|\,S_N\,| &\leqslant 2\,|\,xz\,|\,(V_3V_0)^{1/2} + 2\,|\,yw\,|\,(A_3A_0)^{1/2}. \\ 2\,|\,D_N\,| &\leqslant K\,|\,xw\,|\,(V_3A_0)^{1/2} + K\,|\,yz\,|\,(A_3V_0)^{1/2}. \end{aligned} \tag{4.12}$$

Replacing V_3 and A_3 by their upper bounds V_{3M} given in (3.12), and V_0 and A_0 by their upper bounds given in (4.10), we get the desired constraints:

$$\begin{aligned} |\,x\,| + |\,y\,| &\geqslant \frac{|\,S_N\,|}{(V_{3M}\,\gamma_2)^{1/2}}, \\ |\,x\,| + |\,y\,| &\geqslant \frac{2}{K}\,\frac{|\,D_N\,|}{(V_{3M}\,\gamma_2)^{1/2}}. \end{aligned} \tag{4.13}$$

If it turns out that V_{3M} is larger than V_{cm} defined in eq. (3.19), then these bounds can be improved, as was discussed in section 3.3, by replacing V_{3M} both in eq. (4.9) and inequalities (4.13) by V_{cm}.

Regarded as bounds on x and y, the inequalities (4.13) are quite involved. Nevertheless they are very important as they constitute all the model-independent information that can be extracted from a knowledge of $\sigma_N(\nu^{\pm}p)$ and $\sigma_N(\nu^{\pm}n)$. The inequalities (4.13) contain not only the obvious lower bounds on $|x|$ and $|y|$, but also upper bounds on $|x|$ and $|y|$. In fact, the requirement of reality of the radical occurring in the definition of γ_2 in eq. (4.11) leads precisely to our octagonal upper bounds (3.15). Thus the region in the xy plane allowed by the inequalities (4.13) is expected to be a bounded region with a hole at the center around the origin provided either S_N or D_N does not vanish.

However, as we have already discussed the upper bounds in the preceding section and also since we do not yet have data on S_N and D_N, we shall restrict ourselves to illustrating the lower bounds implied by the inequalities in (4.13). For this purpose we shall replace γ_2 by its maximum possible value $2\Sigma_N$ and thus obtain the weaker versions of (4.13):

$$|x| + |y| \geqslant \frac{|S_N|}{(2\Sigma_N V_{3M})^{1/2}} \tag{4.14}$$

$$|x| + |y| \geqslant \frac{2}{K} \frac{|D_N|}{(2\Sigma_N V_{3M})^{1/2}} .$$

These inequalities imply that, provided S_N and D_N are nonvanishing, a diamond-shaped region in the xy-plane around the origin is scooped out. Since no data on S_N and D_N are available at the present moment, we cannot plot these lower bounds on S_N and D_N. However, if we take the hypothetical values $|\tilde{S}_N| = \tilde{\Sigma}_N$ or $|\tilde{D}_N| = 1/2\ \tilde{\Sigma}_N$, allowed by the inequalities

$$|S_N| \leqslant \Sigma_N$$

$$|D_N| \leqslant \frac{K}{2} \Sigma_N$$

which follow from simple manipulations of eq. (3.4) and the inequalities (4.12), then, the diamond-shaped region is as indicated in figure 7 for the total cross section data assuming scaling. We should stress that the lower bounds indicated by the diamond-shaped region in figure 7 are *hypothetical* and they should be replaced by the genuine bound, once data on S_N and D_N are available.

A detailed plot of the better inequalities (4.13), which contain both the upper and lower bounds on the values of x and y, will have to await the experimental data on neutral current cross sections of neutrinos and antineutrinos on protons and neutrons separately. We should also remark that whereas the upper bound given in (3.15) can be proved to be the best ones with the given in-put data, no such proof is available for the lower bound contained in (4.13).

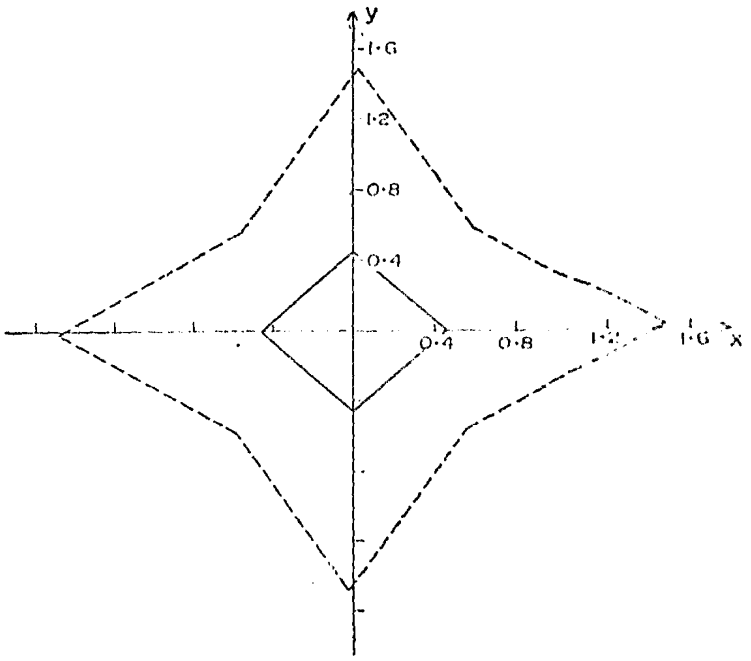

Figure 7. Schematic representation of the lower bounds (4·14) for hypothetical values of S_N and D_N (see text). Values of x and y lying within the diamond-shaped region are forbidden. The broken line is the octagonal upper bound of eq. (3·15′) for $K_t = 1$, show here for comparison.

5. Summary and discussions

We have derived the consequences of the twin assumptions that the neutral weak current consists of only vector and axial-vector currents and that the isovector part of the neutral current is related to that of the charged current by isospin rotation. The results have been given in the form of bounds satisfied by the isovector coupling constants x and y of the neutral current. The upper bounds for x and y utilize neutrino cross sections only for isospin-averaged nucleon whereas the lower bounds for x and y require a knowledge of the cross sections for proton and neutron separately.

The evaluation of these bounds require data on inclusive neutrino scattering experiments either in the form of double differential cross sections or total cross sections. In the case of double differential cross sections our results are quite general as their derivation is independent of any dynamical assumption. For total cross sections we have a choice: bounds which are not so restrictive but assumption-free, and bounds which are very stringent but depend on the validity of Bjorken scaling.

For numerical illustrations we have used only the bounds involving total cross sections. Use of the bounds with differential cross sections should be reserved for the future. It should be emphasized that our bounds can also be used for exclusive cross sections, such as elastic and quasi-elastic neutrino scattering, single pion production processes, as well as for partially integrated cross sections. The only requirement is that the neutral current cross sections Σ_N, Δ_N and the charged current cross sections Σ_C, Δ_C should refer to related reactions in each of which a sum over the charge states of the final hadronic system is understood.

The bounds obtained in this paper do not involve the isoscalar coupling constants z and w. One can study the limitations on these couplings only if the isoscalar currents are related to the isoscalar currents occurring in some other physical processes. In our considerations so far it had not been necessary to define the normalization of the $v_\lambda{}^0$ and $a_\lambda{}^0$ relative to $v_\lambda{}^3$ and $a_\lambda{}^3$ and hence z and w could well have been absorbed into $v_\lambda{}^0$ and $a_\lambda{}^0$. Since the bounds were obtained by eliminating isoscalar contributions, z and w disappear along with $v_\lambda{}^0$ and $a_\lambda{}^0$. It is worth mentioning that a natural, but nonetheless additional, assumption is to relate $v_\lambda{}^0$ to the isoscalar electromagnetic current from which it is possible to derive bounds involving z in addition to x and y (Rajasekaran and Sarma 1975).

Finally we shall discuss the important question: how good are the bounds derived in this paper? We shall restrict our comments to the upper bounds implied by the octagonal inequalities. These inequalities (3.15) are consequences of two basic inequalities; the nonlinear inequality (2.12) for the isovector parts and the linear inequality (2.17) for the isoscalar parts with $\lambda = z$ and $\mu = w$. As noted in section 3.5, the closeness of the experimental value of R_C to 1/3 indicates that the nonlinear inequality (2.31) constraining the isovector contributions is almost an equality at high energies. To that extent, the octagonal bound can be regarded as a tight bound. The loosening of the bound due to the use of the linear inequality (2.33) for the isoscalar contributions could be avoided provided some additional assumption is made such as the relationship of v^0 with the isoscalar electromagnetic current referred to in the previous paragraph. The resulting inequalities involving x, y and z will then be so tight that they may even become equalities, as will be elaborated upon in a subsequent paper. On the other hand, without making any such assumption, the octagonal bounds are the best that can be obtained, as we have shown in the appendix through a variational procedure. Thus, we may conclude that the octagonal inequalities derived in this paper constitute the most stringent bounds on the isovector coupling constants of the neutral current that can be obtained in a general model independent framework.

Appendix

It is the purpose of this appendix to demonstrate that the octagonal inequality (3.15) is the best one under the given input by deriving it from a variational procedure. Our notation here will, to a large extent, conform to that of the subsection 2.3. We start by rewriting eq. (2.11) in a compact form:

$$V_3 = \sum_n{}' \left[v_n{}^3 v_n{}^{3*} + u_n{}^3 u_n{}^{3*}\right]$$

$$A_3 = \sum_n{}' \left[a_n{}^3 a_n{}^{3*} + b_n{}^3 b_n{}^{3*}\right]$$

$$I_3{}^3 = -K \sum_n{}' \mathrm{Re}\,(v_n{}^3 a_n{}^{3*})$$

where

$$v_n^3 \equiv (2a_1 D)^{1/2} \sum_{\lambda}{}'' \langle n, q, \lambda - 1 \mid v_x^3 \mid p, o, \lambda \rangle$$

$$a_n^3 \equiv (2a_1 D)^{1/2} \sum_{\lambda}{}'' \langle n, q, \lambda - 1 \mid a_x^3 \mid p, o, \lambda \rangle$$

$$u_n^3 \equiv \left(\frac{a_2 D}{2}\right)^{1/2} \sum_{\lambda}{}'' \langle n, q, \lambda \mid v_z^3 \mid p, o, \lambda \rangle$$

$$b_n^3 \equiv \left(\frac{a_2 D}{2}\right)^{1/2} \sum_{\lambda}{}'' \langle n, q, \lambda \mid a_z^3 \mid p, o, \lambda \rangle.$$

The isoscalar parts V_0, A_0, I_0^0 can also be concisely expressed in a similar manner in terms of v_n^0, a_n^0, u_n^0, b_n^0.

In terms of these current matrix elements we may now express the neutrino cross-section combinations eqs (3.2)–(3.5) as follows:

$$2\Sigma_N = \sum_n{}' [x^2 (|v_n^3|^2 + |u_n^3|^2) + y^2 (|a_n^3|^2 + |b_n^3|^2) + z^2 (|v_n^0|^2 + |u_n^0|^2) + w^2 (|a_n^0|^2 + |b_n^0|^2)] \quad (A.1)$$

$$2\Delta_N = -K \sum_n{}' [xy \operatorname{Re}(v_n^3 a_n^{3*}) + zw \operatorname{Re}(v_n^0 a_n^{0*})] \quad (A.2)$$

$$\Sigma_C = \sum_n{}' [|v_n^3|^2 + |a_n^3|^2 + |u_n^3|^2 + |b_n^3|^2] \quad (A.3)$$

$$\Delta_C = -K \sum_n{}' \operatorname{Re}(v_n^3 a_n^{3*}) \quad (A.4)$$

Our problem is to obtain bounds on the coupling parameters $x, y, \ldots$ such as to satisfy the relations (A.1)–(A.4). We shall, equivalently, choose to obtain bounds on $2\Sigma_N$ defined by (A.1) under the constraints (A.2)–(A.4), by using the method of Lagrange multipliers. For this purpose we define the Lagrange function

$$L \equiv 2\Sigma_N + \lambda_2 [2\Delta_N + K \sum_n{}' \{xy \operatorname{Re}(v_n^3 a_n^{3*}) + zw \operatorname{Re}(v_n^0 a_n^{0*})\}] + \lambda_3 [\Sigma_C - \sum_n{}' \{|v_n^3|^2 + |a_n^3|^2 + |u_n^3|^2 + |b_n^3|^2\}] + \lambda_1 [\Delta_C + K \sum_n{}' \operatorname{Re}(v_n^3 a_n^{3*})] \quad (A.5)$$

where λ_2, λ_3 and λ_4 are Lagrange multipliers which are real parameters and for Σ_N we should substitute from eq. (A.1).

Extremization of L with respect to the set of 16 variables, $v_n^{3,0}$, $a_n^{3,0}$, $u_n^{3,0}$, $b_n^{3,0}$ and their complex conjugates, leads to the following conditions:

$$2(x^2 - \lambda_3) v_n^3 + K(\lambda_2 xy + \lambda_4) a_n^3 = 0 \quad (A.6)$$

$$2(y^2 - \lambda_3) a_n^3 + K(\lambda_2 xy + \lambda_4) v_n^3 = 0 \quad (A.7)$$

$$(x^2 - \lambda_3)\, u_n^3 = 0 \tag{A.8}$$

$$(y^2 - \lambda_3)\, b_n^3 = 0 \tag{A.9}$$

$$2z^2\, v_n^0 - K\lambda_2 w a_n^0 = 0 \tag{A.10}$$

$$2w^2\, a_n^0 - K\lambda_2 z v_n^0 = 0 \tag{A.11}$$

$$z^2\, u_n^0 = 0 \tag{A.12}$$

$$w^2\, b_n^0 = 0 \tag{A.13}$$

and eight more conditions which are merely complex conjugates of the above equations, and hence need not be considered separately.

Before we proceed to solve the above equations, it is worth noting that we should avoid those solutions which require the vanishing of any of the λ's. For, vanishing of a particular λ_i corresponds to not using the i-th constraint at all and the resulting bound will therefore be a weaker one. More generally, we should avoid solutions of the above equations which demand relations of the type

$$\sum_i C_i \lambda_i = 0 \tag{A.14}$$

where C's are constants independent of the λ's.

Equation (A.8) immediately implies that $u_n^3 = 0$; because if we were to require $x^2 = \lambda_3$ then from (A.6) we have either $\lambda_2 xy = \lambda_1 = 0$ which is of the form (A.14) and hence unacceptable, or $a_n^3 = 0$ which is inconsistent with a nonvanishing Δ_C. Similar reasoning with (A.9) yields $b_n^3 = 0$, while eqs (A.12) and (A.13) trivially imply that the corresponding isoscalar parts also vanish:

$$u_n^0 = b_n^0 = a_n^3 = b_n^3 = 0. \tag{A.15}$$

Thus the solution which extremizes the function defined in (A.5) must have all the scalar matrix elements set zero, a fact which has an obvious parallel in the omission of positive-definite scalar terms, in eq. (2.11).

We next come to the eqs (A.6), (A.7), (A.10) and (A.11). For a nontrivial solution of the transverse variables $v^{3,0}$, $a^{3,0}$ the λ's have to satisfy the following two determinantal conditions:

$$4(x^2 - \lambda_3)(y^2 - \lambda_1) - K^2(\lambda_2 xy - \lambda_1)^2 = 0 \tag{A.16}$$

$$K^2 \lambda_2^2 = 4. \tag{A.17}$$

We are thus left with two relations among the four variables

$$a_n^3 = \frac{2(x^2 - \lambda_3)}{K(\lambda_2 xy - \lambda_1)}\, v_n^3 \tag{A.18}$$

$$a_n^0 = \frac{2z}{K\lambda_2 w}\, v_n^0. \tag{A.19}$$

The procedure now is to use the four eqs (A.16)–(A.19) together with the three constraint equations (A.2)–(A.4) to determine the four variables $v^{3,0}$, $a^{3,0}$ as well as the three parameters λ_2, λ_3, λ_4. Actually only sums of the bilinear products

of the matrix elements can be determined and these alone are relevant for our purpose. Substitution of (A.18) and (A.19) into (A.4) and (A.2) gives

$$\sum_n{}' \mid v_n{}^3 \mid^2 = \frac{\lambda_2 xy + \lambda_1}{2(x^2 - \lambda_3)} \triangle_C \tag{A.20}$$

$$\sum_n{}' \mid a_n{}^3 \mid^2 = \frac{2(x^2 - \lambda_3)}{K^2(\lambda_2 xy + \lambda_1)} \triangle_C \tag{A.21}$$

$$\sum_n{}' \mid v_n{}^0 \mid^2 = \frac{\lambda_2}{2z^2}(2\triangle_N - xy\triangle_C)$$

$$= \frac{1}{Kz^2} \mid 2\triangle_N - xy\triangle_C \mid \tag{A.22}$$

$$\sum_n{}' \mid a_n{}^0 \mid^2 = \frac{2}{w^2 K^2 \lambda_2}(2\triangle_N - xy\triangle_C)$$

$$= \frac{1}{Kw^2} \mid 2\triangle_N - xy\triangle_C \mid. \tag{A.23}$$

Substitution of these in the constraint (A.3) and use of (A.16) yields an equation involving λ's:

$$K^2(\lambda_2 xy + \lambda_1)\ \Sigma_C = 2(x^2 + y^2 - 2\lambda_3)\ \triangle_C. \tag{A.24}$$

With the help of the three eqs (A.16), (A.17) and (A.24) we can now determine the three Lagrange multipliers λ_2, λ_3, λ_4 in terms of Σ_C, $\triangle_C$ and $\triangle_N$. Substituting for them in (A.20)–(A.23) we determine $\Sigma \mid v \mid^2$, etc., which when inserted into (A.1) give us the extremum of Σ_N,

$$\left(\sum_N\right)_{\text{ext}} = \frac{\Sigma_C}{4}\left[x^2 + y^2 \mp (x^2 - y^2)\left(1 - \frac{4\triangle^2_C}{K^2\Sigma^2_C}\right)^{\frac{1}{2}}\right]$$

$$+ \frac{1}{K} \mid 2\triangle_N - xy\triangle_C \mid. \tag{A.25}$$

It may be noted that the two possibilities of the sign above arise from the two possible values of λ_3:

$$2\lambda_3 = -(x^2 + y^2) \pm (x^2 - y^2)\left(1 - \frac{4\triangle^2_C}{K^2\Sigma^2_C}\right)^{-\frac{1}{2}}. \tag{A.26}$$

To ascertain whether this extremum corresponds to a maximum or minimum we have to examine the second derivatives of L with respect to the matrix elements $v_n{}^{3,0}$, etc. The matrix J formed by the second derivatives consists of the following pieces:

Using for brevity the notation,

$$L''(\alpha, \beta) \equiv \frac{\partial^2 L}{\partial\alpha\,\partial\beta^*}$$

$$\begin{pmatrix} L''(v^3, v^3) & L''(v^3, a^3) \\ L''(a^3, v^3) & L''(a^3, a^3) \end{pmatrix} = \begin{pmatrix} x^2 - \lambda_3 & K(\lambda_2 xy + \lambda_4)/2 \\ K(\lambda_2 xy + \lambda_4)/2 & y^2 - \lambda_3 \end{pmatrix} \tag{A.27}$$

$$\begin{pmatrix} L''(v^0, v^0) & L''(v^0, a^0) \\ L''(a^0, v^0) & L''(a^0, a^0) \end{pmatrix} = \begin{pmatrix} z^2 & K\lambda_2 zw/2 \\ K\lambda_2 zw/2 & w^2 \end{pmatrix} \tag{A.28}$$

$$L''(u^3, u^3) = x^2 - \lambda_3 \tag{A.29}$$

$$L''(b^3, b^3) = y^2 - \lambda_3 \tag{A.30}$$

$$L''(u^0, u^0) = z^2 \tag{A.31}$$

$$L''(b^0, b^0) = w^2. \tag{A.32}$$

All other second derivatives of L are zero. Consequently, the nontrivial part of the second-derivative matrix J is a 8×8 matrix having a block-diagonal form comprizing of two 2×2 blocks along the diagonal given by (A.27) and (A.28) and four diagonal elements given by (A.29)-(A.32).

The eight eigenvalues of the matrix J can easily be listed—

$$(x^2 + y^2 - 2\lambda_3), 0, (z^2 + w^2), 0, (x^2 - \lambda_3), (y^2 - \lambda_3), z^2, w^2. \tag{A.33}$$

Barring the particular values $z = w = 0$ (which correspond to specific models), we conclude that due to the presence of the third and the last two eigenvalues above, the matrix J cannot be negative-definite. In other words the extremum (A.25) cannot refer to a maximum. This is obvious otherwise also from the structure of the expression for Σ_N. We can imagine Σ_N to be arbitrarily large by choosing large values for the parameters $|u^0|$ and $|b^0|$ in eq. (A.1) which are unrestricted for any given set of values of Δ_N, Δ_C, and Σ_C.

The necessary condition for the extremum to be a minimum is that all the eigenvalues are non-negative at the point of extremum. This implies the two conditions

$$x^2 \geqslant \lambda_3 \tag{A.34}$$

$$y^2 \geqslant \lambda_3 \tag{A.35}$$

which will be satisfied if we choose the upper (lower) sign in the formula (A.26) for λ_3 when $x^2 - y^2 > 0 (< 0)$. We therefore conclude that the extremum we obtained is a minimum,

$$\Sigma_N \geqslant (\Sigma_N)_{\text{ext}}, \tag{A.36}$$

provided we choose for $x^2 > y^2 (x^2 < y^2)$ the upper (lower) sign in eq. (A.25). The inequality (A.36) is the octagonal inequality (3.15).

For obtaining the bounds involving the total cross sections $\tilde{\Sigma}_N$, $\tilde{\Delta}_N$, $\tilde{\Sigma}_C$, and $\tilde{\Delta}_C$, the integrals over Q^2 and ν may be regarded as sums over discrete values of Q^2 and ν and then the above variational procedure can be followed. One then finds that there are many minima of $\tilde{\Sigma}_N$ which are given by the same expression (A.25) written in terms of total cross sections, each minimum corresponding to the function K evaluated at any given pair of values of the kinematic variables Q^2 and ν. However, only the absolute or the lowest minimum of $\tilde{\Sigma}_N$ is relevant for us and this is obtained for the maximum value of K, namely 2. Thus we recover the bound (3.15′) evaluated for $K_t = 2$. If Bjorken scaling is used, however, the y-integration can be done as before and we get the stronger bound (3.15′) with K_t replaced by unity.

References

Adler S L and Tuan S F 1975 *Phys. Rev.* **D11** 129

Albright C H 1973 *Phys. Rev.* **D8** 3162

Aubert B *et al* 1974 *Phys. Rev. Lett.* **32** 1457

Barish B C *et al* 1975 *Phys. Rev. Lett.* **34** 538

Bég M A B and Zee A 1973 *Phys. Rev. Lett.* **30** 675

Benvenuti A *et al* 1974 *Phys. Rev. Lett.* **32** 800

Bjorken J D 1969 *Phys. Rev.* **179** 1547

Bjorken J D and Paschos E A 1970 *Phys. Rev.* **D1** 3151

Budny R and Scharbach P N 1972 *Phys. Rev.* **D6** 3651

Eichten T *et al* 1973 *Phys. Lett.* **46 B** 274

Gourdin M 1975 Lectures given at the International School of Subnuclear Physics "Ettore Majorana"—Erice (Italy) Preprint PAR–LPTHE 75.18

Hasert F J *et al* 1973 *Phys. Lett.* **46 B** 121 138

Hasert F J *et al* 1974 *Nucl. Phys.* **B73** 1

Kendall H W 1972 in *Proc. Int. Symp. Electron and Photon Interactions at High Energies*, 1971 Ed. N. B Mistry Cornell Univ. Press, N.Y. 1972) p 248

Lee T D and Yang C N 1962 *Phys. Rev.* **126** 2239

Mathur V S, Okubo S and Kim J E 1975 *Phys. Rev.* **D11** 1059

Morfin J G 1975 *Proc. Int. Symp. on Lepton and Photon Interactions at High Energies*, Stanford, California, Ed. W T Kirk (SLAC, Stanford, 1976) p. 537

Pais A and Treiman S B 1972 *Phys. Rev.* **D6** 2700

Pakvasa S and Tuan S F 1974 *Phys. Rev.* **D9** 2698

Palmer R B 1973 *Phys. Lett.* **46 B** 240

Paschos E A and Wolfenstein L 1973 *Phys. Rev.* **D7** 91

Paschos E A and Zakharov V I 1973 *Phys. Rev.* **D8** 215

Rajasekaran G and Sarma K V L 1974 *a Pramāṇa* **2** 62, 225

Rajasekaran G and Sarma K V L 1974 *b Pramāṇa* **3** 44

Rajasekaran G and Sarma K V L 1975 *Phys. Lett.* **55B** 201

Riazuddin and Fayyazuddin 1972 *Phys. Rev.* **D6** 2032

Sakurai J J 1974 *Phys. Rev.* **D9** 250

Sakurai J J 1975 *Neutral Currents Without Gauge Theory Prejudices* CERN preprint TH 2099 (December 1975)

Salam A 1968 in *Elementary Particle Theory*, ed. N Svartholm (Almquist and Wiksells, Stockholm) p. 367

Sehgal L M 1973 *Nucl. Phys.* **B65** 141

Sehgal L M 1974 *Phys. Lett* **48B** 133

Sehgal L M 1975 *Phenomenology of Neutrino Reactions* Argonne preprint ANL–HEP–PR–75–45

Weinberg S 1967 *Phys. Rev. Lett.* **19** 1264

Weinberg S 1972 *Phys. Rev.* **D5** 1412